

PROMIENIOWANIE GENEROWANE PRZEZ NISKOTEMPERATUROWĄ NISKOCIŚNIENIOWĄ PLAZMĘ JARZENIOWĄ I JEGO WPŁYW NA WODĘ, A TYM SAMYM NA STYL I KOMFORT ŻYCIA

Radiation generated by low-temperature low-pressure glow plasma and its effects on water and hence on the life style and comfort

KAREN KHACHATRYAN¹, ZDZISŁAW OSZCZĘDA², JACEK A. SOROKA³, PIOTR TOMASIK²

¹Laboratory of Nanomaterials and Nanotechnology, Faculty of Food Technology, University of Agriculture

²Nantes Nanotechnological Systems

³Scientific Society of Szczecin

Streszczenie/Abstract

Wstęp. W badaniach zidentyfikowano podstawowe mechanizmy związane ze zmianami makrostruktury wody pod wpływem niskotemperaturowej, niskociśnieniowej plazmy jarzeniowej. Niewidzialne długofalowe promieniowanie plazmowe okazało się ważne.

Wyniki. Wykrywalna fala o częstotliwości ok. 1,5 MHz powoduje restrukturyzację tylko w obecności katalizatora – zwilżalnej powierzchni szkła. Przedstawiono generator tej fali, nadający się do modyfikacji wody. Fale częstotliwości terahercowej znacznie szybciej restrukturyzują wodę bez użycia katalizatora. Są one emitowane ze wzbudzonych stanów rotacyjnych zjonizowanych gazów w zastosowanej lampie plazmatronowej.

Metody badawcze. Obliczenia dla rotatorów niesztynnych odpowiadają trwałości wiązań wodorowych.

Wnioski. Obecność fal megahercowych wskazuje na pojawienie się naturalnego mieszacza fal, czyli układu heterodynowego. Sposób, w jaki promieniowanie to oddziałuje z wodą, rozbijając istniejące struktury i tworząc nowe, proponuje się nazwać kalejdoskopią, nawiązując do idei znanej dziecięcej zabawki.

Introduction. The research identifies the basic mechanisms related to changes in the macrostructure of water under the influence of low-temperature, low-pressure glow plasma. Invisible long-wave plasma radiation has proven to be important.

Results. A detectable wave with a frequency of approx. 1.5 MHz causes restructuring only in the presence of a catalyst – a wettable glass surface. A generator of this wave, suitable for water modification, is presented. Terahertz frequency waves restructure water much faster without the use of a catalyst. They are emitted from the excited rotational states of ionized gases in the plasmatron tube used.

Research methods. The calculations for non-rigid rotators correspond to the durability of hydrogen bonds.

Conclusions. The presence of megahertz waves indicates the emergence of a natural wave mixer, i.e. a heterodyne system. The way in which this radiation interacts with water, by breaking down existing structures and creating new ones, is proposed to be called kaleidoscoping, referring to the idea of a well-known children's toy.

Słowa kluczowe: fale terahercowe; niesztynny rotator cząsteczkowy; promieniowanie plazmy; układ heterodyny.

Key words: heterodyne system; non-rigid molecular rotators; plasma radiation; terahertz waves.

1. Introduction

Low energy, low pressure glow plasma, Elkin [10], Reszke [17] (LPGP) when generated electrically near water samples, does not initiate any chemical reactions, Białopiotrowicz [1], Chwastowski [4], Ciesielska [6, 7]. Water treated with LPGP in the air, under nitrogen, oxygen, carbon dioxide, ammonia, methane or argon splits into small clusters and excites molecules of gases dissolved in the water. The latter can then enter smaller aqueous clusters as guests.

Water under plasmatron radiation changes its properties, becoming better absorbed by living organisms, both plant and animal. It improves hydration of the human body, positively affecting the quality of life, Tomasik et al. [1–7].

Since the production of LPGP requires very low pressure, even at low temperatures, water cannot exist in a liquid state. Therefore, water and aqueous solutions must not be exposed directly to LPGP.

In the initial study, the water was placed in tightly sealed vessels of an industrial plasmatron with a conical chamber. Its shape reduced the volume of the chamber three times compared to the cylindrical chamber, which only allowed for faster generation of the required vacuum, Chwastowski [5].

The term „plamed” seemed rational to describe this procedure. In subsequent experiments, the water was treated by placing it 2–3 cm outside the cylindrical glass tube of the plasmatron, Ciesielska [8]. This procedure could be called „plasmatroning”. Hence, the water produced can be called plasmatron water. However, based on the experiments described in this report, which take into account the macrostructure of water, we suggest calling it kaleidoscoped water. Since the exact effect of LPGP treatment on the macrostructure of water is not yet known, it was decided to investigate.

To avoid potential energy transmission by the light emitted by the plasma, the vessels were wrapped in a black opaque plastic film. Since this did not change the behavior of water, electromagnetic waves were considered the only rational way to transmit energy from the plasmatron to water. As such, our research focused on the generation and operation of electromagnetic waves.

2. Materials and Methods

2.1 Materials

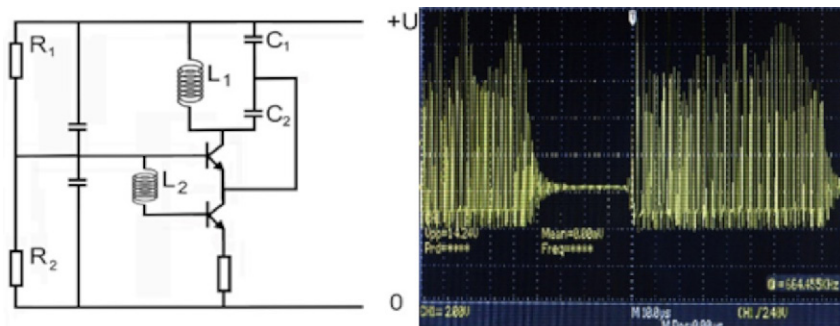


Fig. 1. The general electrical system of the generator tested and the oscillogram of one of the types of generated electromagnetic waves

Municipal water from the Rudna Water Treatment Plant in Cracow (medium hard) -17° dH was used; pH - 7.7, specific conductivity at 25°C - $649\ \mu\text{S}/\text{cm}$, minerals (mg/L): total - 365, Ca - 88, Mg - 10, K - 3.8, Fe(II)/Fe(III) - < 0.025 , and anions: sulphate, carbonate and chloride, ZUW [18].

2.2 Glass

The laboratory vessels were made of soda, potassium and boron glass. Crushed glass sizes from $3\div 5\times 10$ mm to 15×1.5 mm were prepared with Pyrex® and Schott Duran®.

2.3 Plasmatrons

The plasmatron is a cylindrical hermetic discharge tube made of 70 mm x 250 mm DURAN® glass, with two flat electrodes at both ends. Dry, clean air from the plasmatron tube was sucked

out until a vacuum of 0.1 mPa was reached, after which a voltage of 900 V was applied, resulting in a glowing violet plasma. The plasmatron tube contained three main components of low-pressure air: nitrogen, oxygen, and argon, the latter making a negligible contribution to the resulting plasma.

The current flowing through the discharge tube was 8 mA, indicating a power consumption of about 7W. At the same time, two sets of 1H18N9T stainless steel electrodes were used, either (i) flat round electrodes with diameters of 60 mm and 10 mm or (ii) two flat round

electrodes with a diameter of 60 mm. The plasmatron was powered from a 230/900 V transformer secondary circuit either directly or through a diode rectifier in a Graetz system. Depending on the experiment, the plasmatron was powered by 900 V DC or 50 Hz, 900 V AC.

2.4 Generator

The generator of our own design (Fig. 1) featured a resonance inductive-capacitive system, consisting of two inductive coils, L_1 and L_2 , coiled on top of each other. The coil, with an intrinsic diameter of 80 mm, provided insertion of a measuring cell of up to 500 mL (Fig. 2).

2.5 Recognition of origin and properties of plamed water

The following 30 min lasting experiments were carried out at room temperature:

i. The plasmatron is equipped with two flat, of a large diameter round electrodes or one small and the other with a large diameter. The generated plasma was of the cylindrical (if both electrodes have the same diameter) or conical shapes (electrodes of different diameters), respectively.

ii. plasmatron was supplied with either AC or DC with or without additional smoothing.

iii. DC supply was replaced with AC supply of identical voltage.

Experiments were performed using either a glass or plastic (PE) containers filled with water.

2.6 Determination of the concentration of dissolved oxygen

The efficiency of the water treatment was determined by measuring the concentration of dissolved oxygen in the treated water. A WTW multi 3510 set with an optical oxygen FDO[®]925 probe (Xylem Analytics, Germany) was used. The Raman spectrum was analysed using a Perkin Elmer MPF-44a (Waltham Mass., USA) spectrofluorimeter to detect any changes.

2.7 Determination of dielectric constant

The concentrated impedance method was used to perform measurements of the static dielectric permittivity. An HP4191A impedance analyzer, with a frequency range of 1MHz-1GHz, was used at a selected frequency of 10MHz.

2.8 Estimation of electromagnetic noise

To measure electromagnetic radiation with a frequency range of 10 Hz to 10 MHz, we used the SIGLENT SDS 1052DL oscilloscope with ROHS 100MHz/600V probe (Siglent Technologies Co. Ltd.). The oscilloscope probe was placed directly on the glass surface of the plasma generator chamber, and the second side of the probe was grounded to the plasmatron corpus.

2.9 Recognizing terahertz waves

Detecting terahertz radiation is a challenging task. The currently available detector, based on the electric conductivity of hydrophilic gels used in electronic hygrometers, appeared insufficiently sensitive. It was expected that a change in the water configuration in the aqueous electrolyte in the gel would result in a change in the electric conductivity. However, the resulting effect was too subtle. Additionally, pyrometric sensors (NiCeRa) used in detectors of movement at room temperature was ineffective. Independent confirmation of the presence of waves with predicted energies is currently unavailable.

3. Results and Discussion

The plasmatron's power supply has an 230/900 V 50Hz transformer and a Graetz rectifier that can be switched

iii. An alternating voltage of the same potential was applied, resulting in a three-fold increase in process efficiency compared to experiment (i).

In all experiments, the electromagnetic radiation emitted by the plasmatron was measured using an oscilloscope equipped with a high-frequency probe, positioned closely to the plasmatron tube and grounded to the mass.

The visible luminescent area provided the most intense signals, while signals around the electrodes were weak. This indicates that the emission originated from the glow plasma, and the Faraday's dark created around the electrode was inactive.

The resulting oscillogram (Fig. 2) showed that the 50 Hz frequency peaks, which were copies of the mains frequency, were accompanied by additional vibrations of about 1.5 MHz responsible for

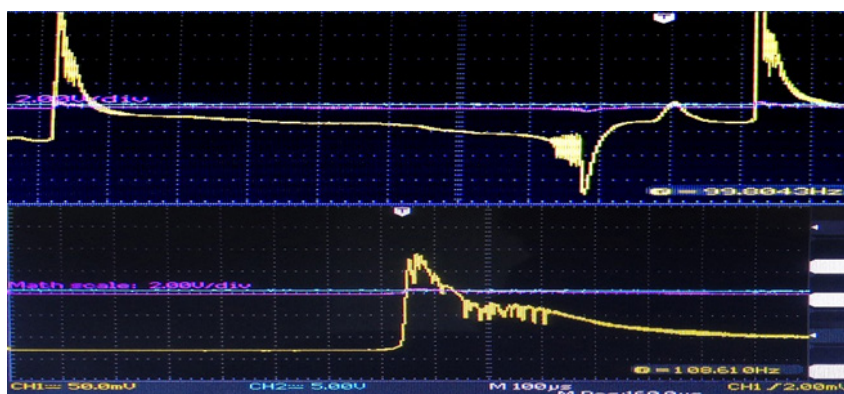


Fig. 2. Oscillogram of plasmatron-generated electromagnetic radiation with visible high-frequency perturbations (AC, 50 Hz).

on or off. Reasons of changes in the properties of the plasma-treated water, were identified in three experiments:

i. The plasma was reshaped from conical to cylindrical (using both electrodes with a large diameter), resulting in a 1.5-fold increase in process efficiency determined by the method described in p. 2.6.

ii. The plasmatron was supplied with a constant, smoothed DC voltage, which caused complete inefficiency of the process.

water restructuring.

Two approaches can provide a concise and precise description of the experimental results, their interpretation, and conclusions.

To test the hypothesis, the plasmatron was replaced by a megahertz electromagnetic wave generator. It made it possible to observe the effect of waves on water in contact with air. A generator was constructed with an inductive capacity resonant system, with an induction coil large enough to accommodate a tank of

treated water. One of several concepts of suitable generators was chosen, Godse [12], which was an original modification of the Colpitts generator. It consists in the use of the main coil (L1) and the auxiliary coil (L2) coiled on top of each other (Fig. 2).

The L1-C system, where $C = C1+C2$, controls the basic generator frequency. The type of radiation generated can be selected by changing the resistances R1 and R2.

Water treated in the generator was placed in either glass or PE containers. The process proceeded very efficiently (determined by the method described in p. 2.6.) in the glass container, whereas in the PE container, it almost completely ceased unless a crushed glass was introduced. In the latter case, the efficiency of the process was considerable and even exceeded that observed in the glass container.

This documents the role of glass as a necessary catalyst for the process. The glass particles were wetted with water, which made their surface transparent to electromagnetic radiation.

The following processes were involved in observed phenomenon:

1. wetting of the glass surface leading to the formation of additional hydrogen bonds with the oxygen atoms bound to silicon or boron atoms in the glass. In the formation of hydrogen bonds a conglomerate of several hydrogen bonded water molecules were involved taking energetically optimal, approximately planar conformation

2. spreading hydrogen bonds with water molecules which did not fit formed structure which generated fragmentation of water into smaller units adhering to the glass surface

3. induced by electromagnetic wave detachment of already existing surface structures accompanied by energetic stabilization. The latter resulted in the formation of new kinds of clathrates, eventually with molecules of dissolved gases as guest molecules.

During the action of electromagnetic radiation on water, both megahertz in the presence of a catalytic wettable surface (in this case, glass) and terahertz, the existing structures are broken down, a "rubble" is formed. From this "debris chaos" the structures of water are reconstructed, but they are in balance with the environment, which may be different from the one surrounding the water originally used. Thus, its inner image can be, and often is, different from the initial one.

Such behavior of water resembled formation of various graphical structures in kaleidoscopes. Therefore, we propose here to introduce a new term kaleidoscoping for describing way of the water restructuring. That hypothesis itself should be confirmed by computations.

One could compare energy of radio wave of 1.5 MHz with energy of a weak hydrogen bond (4 kcal/mole = 16.76 kJ/mole). Thus

$$E = hv = 1.5 \cdot 10^6 \cdot 6.626 \cdot 10^{-34} = 9.945 \cdot 10^{-28} \text{ J} \quad (1)$$

Energy of that weak hydrogen bond per one water molecule provided $16.76 \cdot 10^3 / 6.02 \cdot 10^{23} = 2.784 \cdot 10^{-20}$ J. However, the use of 1 J energy to shake 10 L of beer causing its rapid foaming requires comparable energy of $1 / (10 \cdot 55.5 \cdot 6.02 \cdot 10^{23}) = 3 \cdot 10^{-27}$ J. Thus, energy of a quant of radio radiation cor-

responded to $3.57 \cdot 10^{-6}$ % of energy of the hydrogen bond. Such disproportion showed that existing hydrogen bonds could not be perturbed to a considerable degree. Also energy of wetting, e.g. of coals, computed per one water molecule equal to $2.9 \cdot 10^{-21}$ J covered hardly $3.43 \cdot 10^{-5}$ % energy required for injury of hydrogen bonds. Therefore, the effect on water must have a similar mechanism in both cases. Thus far, details of that mechanism remain unknown.

The radiation of the plasmatron has a very strong effect on the microstructure of water. Larger clusters break down into smaller clusters similar to the size of isolated water molecules in order to transform again into large units to provide a balance with the environment, if it has been changed during irradiation. Such a conclusion follows directly from the measurements of the dielectric constant (Fig. 3).

The above measurements, repeated three times, were performed at 20°C for deionized water subjected to 20 minutes of plasmatron radiation.

Based on Onsager's theory, Petrov

$$[9VkT/4\pi N] \left[\frac{(\epsilon_0 - \epsilon_\infty)(2\epsilon_0 + \epsilon_\infty)}{\epsilon_0(\epsilon_\infty + 2)^2} \right] = \mu^2_0 \quad (2)$$

the electric dipole moments of the measured water were estimated (Table 1).

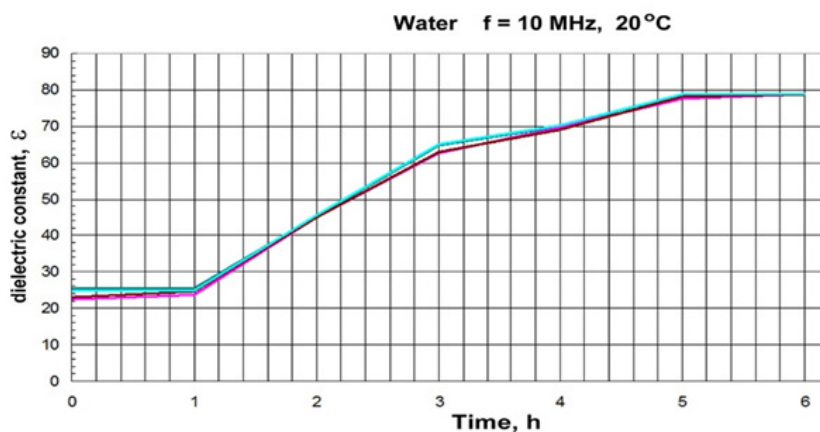


Fig. 3. Changes in the dielectric constant of irradiated deionized water were measured three times, counting from the shutdown of the plasmatron after one hour

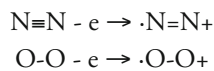
Tab. 1. Time decay of the electric dipole moment of water after stopping plasmotron radiation (PR).

Time after PR [h]	ϵ_{∞}	ϵ_0	μ_0 [D]
1	1.9	25	1.74
3	1.9	63	2.86
4	1.9	70	3.02
5	1.9	78	3.20

The estimated value of 1.74 D is close to the theoretical value of 1.84 D of the isolated water molecule and in our case, means "rubble". Performed experiments revealed that the effectiveness of the generator was measurable but it was essentially lower than that of plasmatron. In case of generator, any considerable restructuring of the water macrostructure required several hours whereas in case of plasmatron such effect was available within few minutes of the treatment.

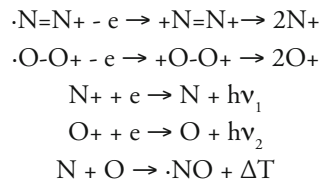
Such effect suggested an involvement of additional, possible main, effect accompanying generation of plasma from two-atom gas such as the air under very low pressure. In clean dry air, only nitrogen and oxygen are important, so further considerations will concern only these two elements in molecular form and the potential product of their mutual chemical reaction - nitric oxide.

It could be an emission from molecular rotational states of their monocations. Symmetric molecules deprived of electric dipole moment as N_2 and O_2 were inactive, but ionised molecules with a large electric dipole moment which could be responsible for their activity. Such molecules were generated in plasmatron according to scheme below.



Subsequent ionization leads to a series of reactions providing ionized atomic nitrogen and oxygen. Both recombined with electrons, emitting light and took atomic forms. Recombination generating molecular forms of nitrogen and oxygen

was strongly inhibited because of low pressure inside plasmatron. Moreover, nitrogen oxide, $\cdot N = O$, a polar molecule active in infrared and rotational spectra, might be new sole detectable product of recombination.



Thus, inertia moments, I , for molecules of N_2 , O_2 and NO

$$I = R^2 \cdot (m_A \cdot m_B) / (m_A + m_B) = mR^2/2$$

If $m_A = m_B = m$

$$\begin{aligned} I(^{14}N_2^+) &= 1.963 \cdot 10^{-46} \text{ kg} \cdot \text{m}^2 \\ I(^{16}O_2^+) &= 2.109 \cdot 10^{-46} \text{ kg} \cdot \text{m}^2 \end{aligned}$$

and if $m_A \neq m_B$

$$I(^{14,16}NO) = 1.698 \cdot 10^{-46} \text{ kg} \cdot \text{m}^2$$

and corresponding levels of zero rotational energy (B) for those molecules were computed employing Eq. (3):

$$B = h^2 / (8\pi^2 \cdot I) \quad (3)$$

States of quantum number of rotation lower by 1 would be exposed to emission from excited rotational states given by Eq. (4).

$$\Delta E(J_{n+1} - J_n) = 2B(J + 1) \quad (4)$$

where J was the rotation quantum number.

Frequency relevant to that energy was available from Eq. (5):

$$\nu = \Delta E/h \text{ [Hz]} \quad (5)$$

Thus:

$$\begin{aligned} \nu(^{14}N_2^+) &= 2 \cdot [2.8325 \cdot 10^{-23} / 6.626 \cdot 10^{-34}] \\ &\cdot (J + 1) = 8.5496 \cdot 10^{10} \cdot (J + 1) \text{ Hz} \end{aligned}$$

and similarly

$$\begin{aligned} \nu(^{16}O_2^+) &= 7.95804 \cdot 10^{10} \cdot (J + 1) \text{ Hz} \\ \nu(^{14,16}NO) &= 4.9422 \cdot 10^{10} \cdot (J + 1) \text{ Hz} \end{aligned}$$

For rotational states determined with subsequent quantum numbers of rotation, J , computations predicted emission of electromagnetic wave of parameters collected in Table 2.

In case of emitted energy and energy of weak hydrogen bonds, the percentage values in Table 1 deal with wetting of coal. Data for wetting of different glasses types were unavailable for us. The real rotating two-atom system involved bond which could be deformed. It was called non-rigid rotator. Its energy could be expressed with Eq. (6)

$$E = BJ(J+1) - DJ^2(J+1)^2 \quad (6)$$

where $D = B^3 / (hv)^2$ was the centrifugal force constant whereas energy of a rigid rotator was given by Eq. (7).

$$E = BJ(J+1) \quad (7)$$

The ν parameter denotes oscillation frequency of atoms along the bond. Since the lack of activity of N_2 and O_2 in the absorption IR spectra that parameter could be taken from the corresponding Raman spectra. Thus, $\bar{\nu}_{N=N} = 2340 \text{ cm}^{-1}$ and $\bar{\nu}_{O-O} = 1510 \text{ cm}^{-1}$, Ohno [14], Petrov

Since monoionized molecules of nitrogen and oxygen took $\cdot N = N^+$ and $\cdot O - O^+$ structures, respectively, the bond force in molecular nitrogen plasma reached 2/3 oscillation energy $E_{\cdot NN^+} = 1568 \text{ cm}^{-1}$. Thus, $\bar{\nu}_{N=N} = 4.704 \cdot 10^{13} \text{ Hz}$, and $\bar{\nu}_{O-O} = 4.530 \cdot 10^{13} \text{ Hz}$ and, therefore, the centrifugal force constant of nitrogen and oxygen took $9.358 \cdot 10^{-29} \text{ J}$ and

Tab. 2. Energy, frequency, wavelength of wave generated by plasma generation of nitrogen, oxygen and nitric oxide molecules and percentage sharing of calculated energies in the wetting energy of hard coal, Buczek

Transition $J_{n+1} \rightarrow J_n$	$^{14}\text{N}_2^+$			$^{16}\text{O}_2^+$			$^{14,16}\text{NO}$	
	ν THz	λ mm	Energy [10^{-22}J] /% of wetting energy	ν THz	λ mm	Energy [10^{-22}J] /% of wetting energy	ν THz	λ mm
2→1	0.1701	1.764	2.266 / 7.8	0.1591	1.885	2.101 / 7.2	0.1972	1.557
3→2	0.3847	0.781	3.399 / 11.7	0.3581	0.838	3.151 / 10.9	0.2965	1.012
4→3	0.5130	0.585	4.532 / 15.6	0.4775	0.628	4.201 / 14.5	0.3954	0.759
5→4	0.6412	0.469	5.665 / 19.5	0.5969	0.503	5.252 / 18.1	0.4942	0.607
6→5	0.7695	0.390	6.790 / 23.4	0.7162	0.419	6.302 / 21.7	0.5931	0.506
7→6	0.8977	0.334	7.931 / 27.3	0.8356	0.359	7.353 / 25.4	0.6919	0.433
8→7	1.0259	0.292	9.064 / 31.2	0.9550	0.314	8.403 / 29.0	0.7907	0.379
9→8	1.1541	0.260	10.197 / 35.2	1.0744	0.279	9.453 / 32.6	0.8896	0.337
10→9	1.2823	0.234	11.330 / 39.0	1.1938	0.251	10.434 / 36.0	0.9884	0.303

$8.137 \cdot 10^{-29}$ J, respectively. In the case of NO, the necessary data were available from the IR spectrum and $\bar{\nu} \cdot \text{N}=\text{O} = 1875 \text{ cm}^{-1}$ was withdrawn from Brix [2]. It should be emphasized that computed values were estimated for electrically neutral molecules whereas in analysed phenomenon participate two types of ions. Their real bond energies could differ from those presented above.

Table 3 collects amendments resulting from non-rigidity of rotator of the nitrogen and oxygen molecules in corresponding plasmas. They correspond to the transitions between nearest quantum states.

Since energy values emitted from the rigid rotator reached 10^{-22} J calculated amendments of the 10^{-27} J order seemed to be unessential in investigated process.

Emitted waves could again mix with one another providing summed and differential frequencies. The latter could, eventually, be detected because they did not belong to so-called terahertz break.

Emission of few waves of different frequencies usually resulted in interference/mixing similar as in heterodyne concept, and in this moment, we propose to consider them as a natural occurred heterodyne system. Its visibility increased with generated waves coherence. As the

Tab. 3. Amendments of energy emitted from non-rigid rotator.

$J_{n+1} \rightarrow J_n$ n	$D_{\cdot\text{N}=\text{N}^+}$ 10^{-27} J	$D_{\cdot\text{O}=\text{O}^+}$ 10^{-27} J	$D_{\cdot\text{N}=\text{O}}$ 10^{-27} J
1	1.497	1.302	0.555
2	3.369	2.929	1.250
3	5.989	5.208	2.222
4	9.378	8.137	3.472
5	13.745	11.778	4.999
6	18.341	15.949	6.805
7	23.956	20.832	8.888
8	30.319	26.365	11.249
9	37.431	32.550	13.887

result, two waves were generated. Their frequency was a sum and difference of frequencies of their participants, respectively. Considerations presented below focused solely on a difference which lead to lower frequencies, thus residing in a readily detectable range. Relationships quoted above demonstrated that when quantum number declined by 1 energy emitted from non-rigid rotator declines as given by Eq. (8)

$$\Delta E = B(J+1)(J+2) - BJ(J+1) - D(J+1)^2(J+2)^2 + DJ^2(J+1)^2 = 2[B - 2D(J+1)^2](J+1) \quad (8)$$

Interference/mixing of waves emitted on transition from vicinal quantum numbers was given by Eq. (9)

$$\Delta \Delta E = 2[B - 2D(J+2)^2](J+2) - 2[B - 2D(J+1)^2](J+1) \quad (9)$$

Similarly, interference of waves generated on transition from levels of subsequent quantum numbers provided the waves of energy given by Eq. (10)

$$\Delta \Delta E' = 2[B - 2D(J+3)^2](J+3) - 2[B - 2D(J+2)^2](J+2) \quad (10)$$

Under such circumstances subsequent waves of various energy could be gene-

rated. Subsequently, they were capable of interference of the second order. Its energy depended on quantum numbers of rotation and elasticity of rotator as given in Eq. (11)

$$\Delta E^{\text{II}} = 4D[(J+3)^3 - 2(J+2)^3 + (J+1)^3] \\ = 4D \cdot 6(J+2) \equiv 4Df_{(J)} \quad (11)$$

Values of the $f_{(J)}$ function indicating the second order interference for a few quantum numbers

These data revealed that energy of those waves was situated in the range from $\sim 4 \cdot 10^{-27}$ to $\sim 4 \cdot 10^{-26}$ J, and their corresponding frequency was in the range of 6 to 36 MHz. In case of $\cdot\text{NO}$ that range extended from $\sim 1.2 \cdot 10^{-27}$ to $\sim 7 \cdot 10^{-27}$ J what corresponded to 1.8 to 10 MHz. These lower values could exist within the range provided in the spectrum emitted by used plasmatron. Therefore, one might state, that only a triad of rotational states described by rotation quantum numbers ($J \pm 1$, $J > 1$) was involved in described mechanism.

It should be underlined that above considerations dealt with the interference of waves generated from the same kind of molecules. Therefore, they could be described as homomolecular interference, separately for nitrogen and oxygen molecules. When plasma contained simultaneously nitrogen and oxygen a heteromolecular interference could take place. In consequence, number of observed frequencies could increase at least by four times. Actual oscillation frequency of the ionised nitrogen and oxygen remained unknown. If both frequencies would be twice as high as accepted here, computed frequencies would be exactly equal to those observed in operating plasmatron.

That explanation was supported by the fact that in ionized molecules atomic bond was assisted by electrostatic interactions. The latter increased strength of that bond and, for that sake, an increase in the oscillation energy of the ionized molecule was observed.

Tab. 4. Coefficients of homocomponent second order interference and energy of waves generated with ionized molecules of nitrogen and oxygen.

J^*	$f_{(J)}$	ΔE^{II} [J] $\cdot\text{NN}^+$	ΔE^{II} [J] $\cdot\text{OO}^+$	ΔE^{II} [J] $\cdot\text{NO}$
0	12	$4.492 \cdot 10^{-27}$	$3.906 \cdot 10^{-27}$	$1.213 \cdot 10^{-27}$
1	18	$6.738 \cdot 10^{-27}$	$5.859 \cdot 10^{-27}$	$1.820 \cdot 10^{-27}$
2	24	$8.984 \cdot 10^{-27}$	$7.812 \cdot 10^{-27}$	$2.427 \cdot 10^{-27}$
3	30	$1.123 \cdot 10^{-26}$	$9.764 \cdot 10^{-27}$	$3.034 \cdot 10^{-27}$
4	36	$1.348 \cdot 10^{-26}$	$1.172 \cdot 10^{-26}$	$3.640 \cdot 10^{-27}$
5	42	$1.572 \cdot 10^{-26}$	$1.367 \cdot 10^{-26}$	$4.247 \cdot 10^{-27}$
6	48	$1.797 \cdot 10^{-26}$	$1.562 \cdot 10^{-26}$	$4.854 \cdot 10^{-27}$
7	54	$2.022 \cdot 10^{-26}$	$1.758 \cdot 10^{-26}$	$5.461 \cdot 10^{-27}$
8	60	$2.246 \cdot 10^{-26}$	$1.953 \cdot 10^{-26}$	$6.067 \cdot 10^{-27}$
9	66	$2.470 \cdot 10^{-26}$	$2.148 \cdot 10^{-26}$	$6.674 \cdot 10^{-27}$

* Quantum number of lower energetic state

Ceasing of the plasmatron activity was observed when the inlet of fresh air was not provided. Probably, plasmatron ($U = 700\text{-}1000\text{V}$) offered energy of the order of 1 keV which significantly exceeded energy of dissociation of N_2 (9.8 eV) and O_2 (5.2 eV) In a consequence, atomic N and O were formed and under very low pressure the effective recombination to diatomic molecules was suspicious. In the band of rotational energy the monoatomic gases remained inactive. Currently, no practical method of precise detection of waves in this range is

available. Therefore, it is still commonly called as a terahertz gap.

4. Conclusions

Treating water with the radiation produced during the operation of the plasmatron could be called plasmatroning (previously plasmatronics), but taking into account the internal changes in the water, kaleidoscooping seems to be a better name.

This process occurs under the influence of megahertz radiation, which requires a wettable glass surface as a catalyst,

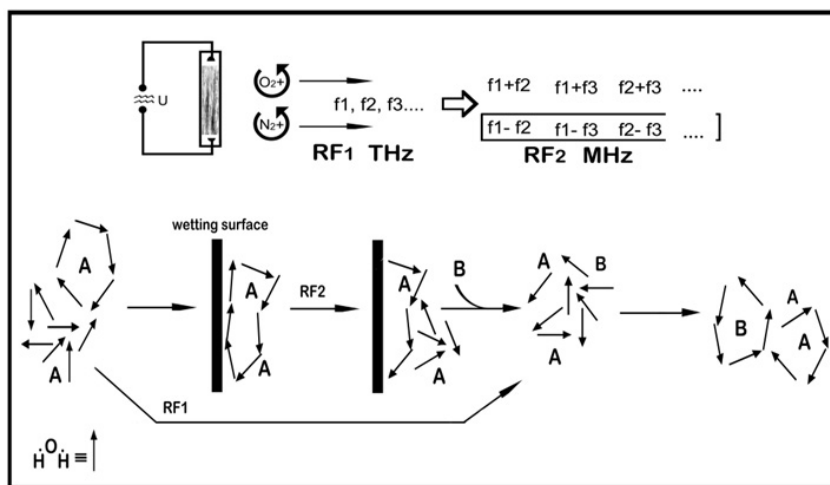


Fig. 4. Schematic illustration of the interaction of terahertz and megahertz radiation in the presence of a wettable surface with water being in contact with air. The synthesis of megahertz frequencies inside plasmatron tube provided natural heterodyne system, with terahertz frequencies mixing corresponding to emissions from different rotational levels.

and terahertz radiation, which does not require a catalyst. Terahertz radiation is generated by the radiation from excited rotational states of nitrogen ions, oxygen, and by-product nitric oxide. The first stage of terahertz radiation involves the breakdown of water clathrates into individual molecules (Figure 4).

This is evidenced by significant changes in the dielectric constant of kaleidoscoped water. New clathrates are generated within a few hours, with their composition depending on the environment. Based on postulated mechanism, megahertz radiation is emitted by excited non-rigid molecular rotators through a self-appearing heterodyne system formed inside a working plasmatron.

Constructing a megahertz wave transmitter is uneconomical due to the requirement of very long antenna (1.5

MHz is a wave length of 200 m, $\lambda/2 = 100$ m), whereas the generator described and tested is compact. However, a plasmatron is still necessary for producing terahertz waves.

To summarize the results of our research, we must emphasize that it is necessary to take into account the health effects of terahertz radiation, which has not yet been considered dangerous. Similarly, the effects on humans of naturally forming plasma, known as the aurora borealis, are also ignored and remain unexplored.

Author Contributions: Conceptualization, J. A. S. and P. T.; methodology, J. A. S.; software, J. A. S.; validation, K. K. and P. T.; formal analysis, J. A. S. and K. K.; investigation, J. A. S., K. K. and Z. O.; resources, Z. O.; writing—original draft preparation, J. A. S. and P. T.;

writing—review and editing, J. A. S., K. K. and P. T.; supervision, P. T. All authors have read and agreed to the published version of the manuscript.

Funding: This research received no external funding.

Data Availability Statement: The data presented in this study are available on request from the corresponding author.

Conflicts of Interest: The authors declare no conflicts of interest.

Address for correspondence
Adres do korespondencji
jacek.soroka@zut.edu.pl

References

- Bax E. B.: Historia Rewolucji Francuskiej (przełoż. T. Białopiotrowicz, T. Ciesielski, W. Domański J., Duskocz, M., Khachatryan, K., Fiedorowicz, M., Graz, K., Kołoczek, H., Kozak, A., Oszczyda, Z. et al.: Structure and Physicochemical Properties of Water Treated with Low-Temperature Low-Frequency Glow Plasma. *Curr. Phys. Chem.* 2016, 6, s. 312–320, doi:10.2174/187794680666616118152613.
- Brix, P., Herzberg, G.: The Dissociation Energy of Oxygen. *J. Chem. Phys.* 1953, 21, s. 2240–2240, doi:10.1063/1.1698843.
- Buczek, B., Wolak, E.: Evaluation of Usability of Adsorbent from Carbonaceous Precursors for Energy Storage System. *Gospod. Surowcami Miner. – Miner. Resour. Manag.* 23, s. 29–39.
- Chwastowski, J., Ciesielska, K., Ciesielski, W., Khachatryan, K., Kołoczek, H., Kulawik, D., Oszczyda, Z., Tomasik, P., Witczak, M.: Structure and Physicochemical Properties of Water Treated under Nitrogen with Low-Temperature Glow Plasma. *Water* 2020, 12, s. 1314, doi:10.3390/w12051314.4.
- Chwastowski, J., Ciesielski, W., Khachatryan, K., Kołoczek, H., Kulawik, D., Oszczyda, Z., Soroka, J. A., Tomasik, P., Witczak, M.: Water of Increased Content of Molecular Oxygen. *Water* 2020, 12, s. 2488, doi:10.3390/w12092488.
- Ciesielska, A., Ciesielski, W., Khachatryan, K., Kołoczek, H., Kulawik, D., Oszczyda, Z., Soroka, J.A., Tomasik, P.: Structure and Physicochemical Properties of Water Treated under Methane with Low-Temperature Glow Plasma of Low Frequency. *Water* 2020, 12, s. 1638, doi:10.3390/w12061638.
- Ciesielska, A., Ciesielski, W., Khachatryan, K., Kołoczek, H., Kulawik, D.; Oszczyda, Z.; Soroka, J.A.; Tomasik, P.: Structure and Physicochemical Properties of Water Treated under Carbon Dioxide with Low-Temperature Low-Pressure Glow Plasma of Low Frequency. *Water* 2020, 12, 1920, doi:10.3390/w12071920.
- Ciesielska, A., Ciesielski, W., Kołoczek, H., Kulawik, D., Kończyk, J., Oszczyda, Z., Tomasik, P.: Structure and Some Physicochemical and Functional Properties of Water Treated under Ammonia with Low-Temperature Low-Pressure Glow Plasma of Low Frequency. *Open Chem.* 2020, 18, s. 1195–1206, doi:10.1515/CHEM-2020-0166/MACHINEREADEABLE-CITATION /RIS.
- Darwent, B. deBaskerville, others: *Bond Dissociation Energies in Simple Molecules*; US Government Printing Office Washington, DC, 1970.
- Elkin, I., Stręk, W., Stręk, S., Oszczyda, Z.: Equipment for Treatment of Water with Plasma, *Polish patent* 216025 B1, 28.02.2014.
- Fedorov, D. V., Sadhukhan, M., Stöhr, M., Tkatchenko, A.: Quantum-Mechanical Relation between Atomic Dipole Polarizability and the van Der Waals Radius. *Phys. Rev. Lett.* 2018, 121, 183401, doi:10.1103/PHYSREVLETT.121.183401/FIGURES/3/MEDIUM.
- Godse, Atul P., Bakshi, U. A.: *Electronic Circuits: Theory, Analysis and Design*; 9789333223485.
- Gregory, J. K., Clary, D. C., Liu, K.; Brown, M. G., Saykally, R. J.: The Water Dipole Moment in Water Clusters. *Science (80-)*. 1997, 275, s. 814–817, doi:10.1126/SCIENCE.275.5301.814/ASSET/9383E1C5-B1D3-483B-80F2-6D7BB0BFFE39/ASSETS/GRAPHIC/SE0574709003.JPEG.
- Ohno, H., Iizuka, Y., Fujita, S.: Pure Rotational Raman Spectroscopy Applied to N₂/O₂ Analysis of Air Bubbles in Polar Firm. *J. Glaciol.* 2021, 67, s. 903–908, doi:10.1017/JOG.2021.40.
- Onsager, L.: Electric Moments of Molecules in Liquids. *J. Am. Chem. Soc.* 1936, 58, s. 1486–1493, doi:10.1021/JA01299A050/ASSET/JA01299A050.FP.PNG_V03.
- Petrov, D. V., Korolev, B. V., Tikhomirov, A. A., Buldakov, M. A., Korolkov, V. A., Matrosov, I. I.: Analyzing Natural Gas by Spontaneous Raman Scattering Spectroscopy. *J. Opt. Technol. Vol. 80, Issue 7, pp. 426-430* 2013, 80, s. 426–430, doi:10.1364/JOT.80.000426.
- Reszke, E., Yelkin, I., Oszczyda, Z.: Plasming Lamp with Power Supply, *Polish patent* 227530, 2017.
- Zakład Uzdatniania Wody Rudawa - Wodociągi Miasta Krakowa - Serwis Internetowy Available online: <https://wodociagi.krakow.pl/o-firmie/infrastruktura/zaklad-uzdatniania-wody-rudawa.html> (accessed on 14 January 2024).